Appl. Magn. Reson. 23, 81–95 (2002)

Applied Magnetic Resonance

Spatial Distribution of Spin-Labeled Trichogin GA IV in the Gram-Positive Bacterial Cell Membrane Determined from PELDOR Data

A. D. Milov[1], R. I. Samoilova[1], Yu. D. Tsvetkov[1], V. A. Gusev[2], F. Formaggio[3], M. Crisma[3], C. Toniolo[3], and J. Raap[4]

[1] Institute of Chemical Kinetics and Combustion, Russian Academy of Sciences, Novosibirsk, Russian Federation
[2] Institute of Mathematics, Russian Academy of Sciences, Novosibirsk, Russian Federation
[3] Biopolymer Research Center, Consiglio Nazionale delle Ricerche, Department of Organic Chemistry, University of Padova, Padova, Italy
[4] Leiden Institute of Chemistry, Gorlaeus Laboratories, Leiden University, Leiden, The Netherlands

Received July 26, 2002

Abstract. Trichogin GA IV is one of the shortest acyclic linear polypeptide antibiotics of fungal origin, characterized by the presence of three α-amino isobutyric acid residues, an N-octanoyl group and an amino alcohol at the C terminus. Its antibiotic activity is generally thought to be based on its self-assembling and membrane-modifying properties. The technique of double electron-electron resonance in electron spin echo is used to study the spatial distribution of spin-labeled [TOAC-4]-trichogin GA IV analog bound to the cell membrane of the Gram-positive bacterium *Micrococcus luteus*. The intermolecular dipole-dipole spin-spin interaction of TOAC spin labels has been experimentally studied at 77 K in glassy dispersions of the spherical cell particles. It is shown that the nonaggregated peptide molecules are distributed at the cytoplasmic membrane. Two possible distribution models are proposed: (i) the peptide molecules are randomly distributed on both inner and outer membrane surfaces with a distance between the surfaces of 7 nm, (ii) the molecules are randomly distributed in a layer up to 2.4 nm from the external surface of the membrane.

1 Introduction

Trichogin GA IV is a member of the so-called lipopeptaibols, all showing antibacterial activity against Gram-positive bacteria [1–3]. In spite of many studies, the molecular mechanisms of the membrane-modifying activities of trichogin are not yet clear. The length of this amphipathic 11-residue helical molecule is clearly too short to overspan the membrane and a pore-forming mechanism of ion conduction seems not to be plausible. Electron spin resonance (ESR) investigations demonstrated that in liposomes trichogin molecules are bound parallel to the mem-

brane surface with its hydrophobic face oriented toward the membrane. It has been suggested that leakage occurs after initial self-association of trichogin molecules in a carpetlike manner [4].

Although a great deal of structural information about peptaibols has been provided by spectroscopic techniques, the application of these techniques to characterize the aggregation state of trichogin in living bacterial cells is hampered by complex spectral data and a low signal-to-noise ratio due to the limited peptide availability. In this respect the use of ESR spectroscopy together with site-directed spin labeling is attractive for both its selectivity and sensitivity of spin probes incorporated into complex systems.

In the past few years methods of continuous-wave (CW) ESR spectroscopy have been exploited to analyze the interaction between trichogin GA IV and the membrane with the stable nitroxide radical of TOAC (2,2,6,6-tetramethylpiperidine-1-oxyl-4-amino-4-carboxylic acid). It has been shown that the sterically hindered Aib residues can be replaced by the rigid TOAC residues without a loss of antibiotic and membrane-modifying properties [4, 5]. In this way it has been established that the long axis of the helical molecule is oriented in the plane of the bilayer with the hydrophobic face of the amphipathic helix exposed towards the hydrophobic pocket of the membrane and the polar face facing the phospholipid headgroup-water interface (Fig. 1).

The pulsed double resonance in electron spin echo (PELDOR) has been used to analyze the structures and mutual arrangement of spin-labeled trichogin GA IV in frozen glassy hydrophobic solutions [6–10]. It was shown that in apolar solvents trichogin forms aggregates that contain about four peptide molecules. Adding polar solvents such as alcohols or dimethyl sulfoxide to the solution leads to the dissociation of the aggregates.

Since trichogin GA IV can modify biological membranes thus potentially manifesting the antibiotic properties, it was interesting to apply the PELDOR technique for studying the peculiarities of the spatial distribution of peptide molecules of this type in cell membranes. It was also of interest to test the possibility to use this experimental method for investigating the spatial distribution of spin-labeled molecules in complex biological systems.

We have selected *Micrococcus luteus* to investigate the structural features of the bound trichogin GA IV molecules since it is one of the best characterized Gram-positive microorganisms, which have been used before in measurements of

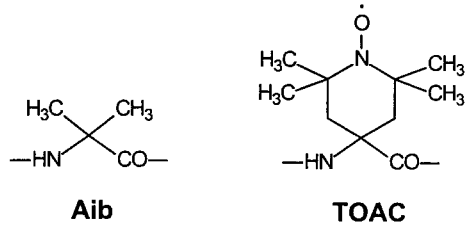

Fig. 1. Structures of native and TOAC-labeled trichogin GA IV peptides.

the K^+ efflux through the cell membrane upon treating them with insect-defensin [11, 12]. The PELDOR technique was used to study the dipole-dipole phase relaxation of spin-labeled peptide TOAC-4 solutions frozen to 77 K in the cell membrane of *M. luteus*. This peptide is the spin-labeled analog of trichogin GA IV in which the Aib residue at the fourth position is substituted by TOAC. In addition, L-leucinol (Lol) is substituted at the C end of trichogin GA IV by L-leucine methyl ether (Leu-OMe). The primary structures of both native and TOAC-labeled trichogin GA IV molecules have the forms

n-Oct-Aib^1-Gly^2-Leu^3-Aib^4-Gly^5-Gly^6-Leu^7-Aib^8-Gly^9-Ile^{10}-Lol^{11} (Trichogin GA IV)

n-Oct-Aib-Gly-Leu-**TOAC**-Gly-Gly-Leu-Aib-Gly-Ile-Leu-OMe (TOAC-4)

The aim of this work is to study the mutual distribution of TOAC-4 molecules in the cell membrane (homogeneous or nonhomogeneous distribution, clusters, aggregates). It might be possible also to elucidate the problem of whether they are located in the membrane volume or on its surface.

2 Experimental

2.1 Preparation of Cells and TOAC-4 Introduction into the Membrane

M. luteus sells, provided by the Centraalbureau voor Schimmelcultures (Utrecht, The Netherlands), were grown to an optical density at 600 nm (OD_{600}) of 1.0 at 37°C in Luria-Bertani medium as described in ref. 11. After centrifugation (at 14000 rpm) cells were carefully resuspended and washed with phosphate buffer (10 mM sodium phosphate and 0.5 M KCl at pH 7.7 with 20% of glycerol added as a cryoprotector). The OD_{600} value of the final cell suspension was 50.

The size distribution of *M. luteus* cells in the samples studied were determined by the flying light scattering indicatrix method (FLSI) [13]. To this end, the cell samples were unfrozen at 0°C and resuspended in fresh buffer containing 10 µl of 10% glucose per milliliter of buffer. The distribution of different radii of the cells studied varied from 250 to 1800 nm. The maximum of the distribution function corresponds to a radius of 500 nm.

The spin-labeled TOAC-4 was synthesized as has been described before [4, 5, 14]. The peptide was introduced into the cell membrane by the following procedure. Phosphate buffer was added to a TOAC-4 solution in ethyl alcohol to a final ratio of 1:1 (v/v). A suspension of cells (OD_{600} = 50) in phosphate buffer was rapidly added to the peptide solution during continuous mixing with the help of a magnetic mixer. After the addition of the cells was completed, the ratio between the alcohol and buffer volumes was 1:2. This solvent mixture was chosen to prevent precipitation of the peptide without damaging the cells [16]. Mixing was continued for the next 5 min. Experimental evidence about the noninvasive influence of the solvent to the integrity of the cell is supported by the absence of any leakage of ^{32}P compounds at low alcohol content, in contrast to a sub-

stantial leakage observed at high alcohol percentages [16]. When equilibrium was achieved, the solvent was removed by centrifuging the cells (14000 rpm for 2 min). After removing the supernatant, the cells were washed two times with fresh buffer and recentrifuged. The supernatant was removed and the residual cell pellet was frozen in an ampoule to perform PELDOR and ESR measurements.The quantitative incorporation of TOAC-4 into the membrane was checked by measuring the ESR spectrum of the cell suspension before and after the binding procedure.

2.2 Background of PELDOR Spectroscopy

The PELDOR method has been described in detail [15, 16]. Two microwave pulses at frequency ω_A induce an electron spin echo (ESE) signal in a spin system. The second pulse is supplied at time τ after the first pulse. The spin echo signal arises at time 2τ after the first pulse. Between 0 and 2τ, a pumping pulse at frequency ω_B is applied at time T after the first pulse. In this method, the spins can be arbitrarily divided into two groups. The spins are labeled as spins A (at ω_A) and spins B excited by the pumping pulse at ω_B. The pumping pulse induces transitions between Zeeman levels of spins B and thus changes local magnetic fields at spins A. This results in additional dephasing of spins A and hence, in a decrease of the ESE amplitude. This decrease depends on the value of the dipole-dipole spin coupling, the time position and intensity of a pumping pulse. The main decay of the ESE signal occurs within a characteristic time $T \sim 1/D$, where D is a typical value of the dipole-dipole spin coupling. Usually, in experiment, time τ between the first and second pulses is fixed and under study is the dependence of the PELDOR signal amplitude V on time T between the first and the pumping pulses.

2.3 ESR and PELDOR Experiments

The samples for ESR and PELDOR experiments were glass ampoules with a diameter of about 0.5 cm containing about 0.1 ml of the solution studied. The samples were frozen by inserting the ampoules into liquid nitrogen.

The ESR spectra of the spin-labeled TOAC-4 peptide were obtained on an ESP-380 Bruker spectrometer at a modulation frequency of 100 kHz and a modulation amplitude of 0.1 mT in the absence of spectrum saturation. To obtain the ESR and PELDOR spectra at 77 K, the samples under study were placed in the finger of a quartz Dewar flask cooled by liquid nitrogen and located in the resonator of a spectrometer.

The PELDOR experiments were carried out on an ESE spectrometer supplied with a bimodal resonator and a device for producing pulses at the pumping frequency [9, 10]. The difference in registration and pumping frequencies was about 100 MHz. Durations of the first and second pulses forming the spin echo were

40 and 70 ns, respectively. The pumping pulse duration was about 40 ns. The value of the probability of spin B rotation by a pumping pulse p_b was determined as described in refs. 8 and 10 from the PELDOR data on the frozen solutions of the double-labeled peptide TOAC-1,8 in ethanol. The p_b value was 0.17.

3 Results

3.1 ESR and PELDOR Spectra of Spin-Labeled Trichogin GA IV Bound to M. luteus Cells

The CW-ESR spectra of TOAC-4 in the cell-bound state are similar to the spectra of TOAC-4 in various solutions when they are recorded at the low-temperature frozen glass state [6–10]. Figure 2 exemplifies the ESR spectrum of the peptide-bound cell suspension frozen to 77 K and containing about 10^6 TOAC-4 molecules per cell. With other peptide contents in the cell, the spectra have a similar shape. Figure 2 also shows the spectrum of TOAC-4 molecules in a glassy (frozen) ethanol solution. As follows, the ESR spectra display no peculiarities in the TOAC-4 distribution in the cell membrane.

More interesting features of the TOAC-4 distribution are observed in PELDOR experiments studying the dipole-dipole relaxation in these systems. Figure 3 shows the dependence of the logarithm of the PELDOR signal V on the position of pumping pulse T for the same systems. Curves 1 and 2 are related to

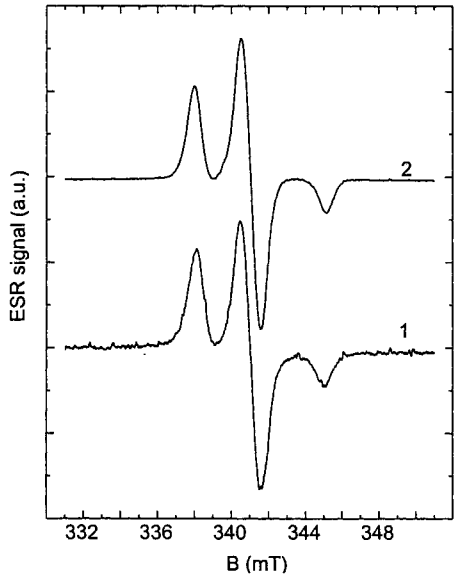

Fig. 2. CW-ESR spectra of TOAC-4 bound to frozen *M. luteus* cells (curve 1) and in the frozen solution of ethanol (curve 2) recorded at 77 K.

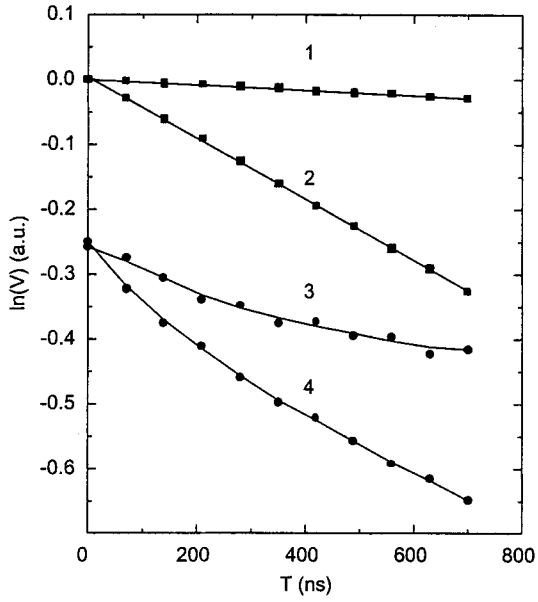

Fig. 3. The experimental $\ln(V)$ on T dependences for TOAC-4 (determined at 77 K): curves 1 and 2, frozen glassy solutions in ethanol, spin label concentrations are $2.7 \cdot 10^{-4}$ M and $2.7 \cdot 10^{-3}$ M, respectively; curves 3 and 4, frozen suspensions (in phosphate buffer) of TOAC-4 bound to *M. luteus* cells, $1.1 \cdot 10^{-4}$ M and $2.8 \cdot 10^{-4}$ M, respectively.

glassy solutions of TOAC-4 in ethanol by two different concentrations of TOAC-4, $2.7 \cdot 10^{-4}$ M and $2.7 \cdot 10^{-3}$ M, respectively. Curves 3 and 4 are obtained for TOAC-4 bound to the cell membrane of *M. luteus* at two different concentrations of TOAC-4 in the probes, $1.1 \cdot 10^{-4}$ M and $2.8 \cdot 10^{-4}$ M, respectively. Figure 3 demonstrates two differences between the PELDOR signal decays for TOAC-4 in the ethanol solution and in the cell suspension: (i) dependences of $\ln(V)$ on T for TOAC-4 in the ethanol solution and in the cell suspension are different; linear dependences of $\ln(V)$ on T are obtained for ethanol solutions and concave curves are obtained for the cell suspensions, (ii) comparison of curves 1 and 4 shows that at about the same mean concentration of TOAC-4, the dipole-dipole relaxation of TOAC-4 in the cell suspension is more efficient than that in the ethanol solution. A similar efficiency is obtained when the spin label concentration in ethanol is about ten times higher compared to the mean concentration of spin labels in the cells (see curves 2 and 4). The linear dependences of $\ln(V)$ on T for TOAC-4 solutions in ethanol denotes the usual exponential dependence which corresponds to a random distribution of peptide molecules in solution. The observed differences in the decay curves and the efficient relaxation of TOAC-4 in cell suspension (in comparison with that in ethanol at the same mean concentrations of the spin labels) denotes that the local concentration of spin labels in the cell suspension is higher than the mean overall concentration.

The local concentration of the spin labels in the cell suspension can be estimated by comparing the amplitudes of the spectral decays measured for the spin concentrations in ethanol and in the cell suspension. Figure 3 shows that the mean decay of curve 2 (TOAC solution in ethanol) is about the same as for curve 4 (TOAC-4 in the cell suspension). Neglecting the difference between the forms of these curves we can say that the mean dipole-dipole interaction between the spin labels is the same in both cases. Thus, the value of the local concentration of TOAC-4 in the cell suspension (curve 4) corresponds to the concentration of TOAC-4 in ethanol (curve 2). This rough estimation shows that the local concentration of TOAC-4 in the cell suspension is ten times higher than the mean concentration. The value of the local concentration in this case is about $2.7 \cdot 10^{-3}$ M which corresponds to a mean distance between spin labels $\langle r \rangle \approx 8$ nm. This value is of the same order of magnitude as the thickness of the cell membrane (see Sect. 4) and it confirms that the TOAC-4 molecules are located at the plasma membrane. More detailed information about the mutual distribution of spin labels in the membrane may be extracted from the form of the PELDOR dependences. Note that in the observed $V(T)$ dependences there is no fast decay of the PELDOR signal at short times T ($T < 100$ ns) characteristic for aggregates of spin-labeled trichogin [8–10].

The nonexponential decays of the PELDOR signal V on T can be conveniently represented as follows [15]

$$V = \exp(-\alpha T^q), \tag{1}$$

where α and q are experimental parameters. According to ref. 15, the value of parameter q depends on the type of mutual arrangement of spin labels. For example, upon a random distribution of spins in the bulk, $q = 1$. However, when they are distributed on a plane, $q = 2/3$. With a random distribution along a straight line, we get $q = 1/3$. Thus, it is expected that by comparing the experimental value of q with those calculated for the different models, one can gain a notion of the pattern of the spatial distribution of spin labels. The value of parameter α depends not only on the type of spatial distribution of spin labels but also on the concentration of spin labels.

Figure 4 shows the experimental curves 1–3 for TOAC-4 in the cell-bound state plotted in the coordinates $\ln(\ln(V))$ vs. $\ln(T)$. The dependencies correspond to different mean concentrations of TOAC-4 in the specimen and therefore to different concentrations of peptide molecules in the membrane. As a result, the experimental data can be described by the dependence of the type of Eq. (1) where parameter $q = 0.71 \pm 0.12$ is independent of the TOAC-4 concentration.

The experimental value of q is close to the value of this parameter upon the spin distribution on a plane ($q = 2/3$). The cell radius R, within the range from 250 to 1800 nm, is much greater than the effective distance for the dipole-dipole interaction of spin labels $\langle r \rangle \approx 8$ nm. When the distances between the spin labels are substantially larger than $\langle r \rangle$, the spins will interact weakly and fail to contribute much to the $V(T)$ decay. In this case, at a distance of the order of

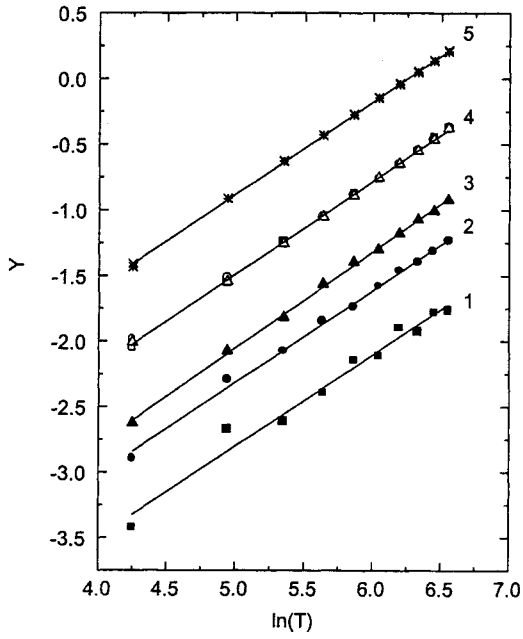

Fig. 4. Experimental and calculated dependences of the PELDOR signal V on T. For the curves 1–3 the ordinate Y is $\ln(-\ln(V))$, while for the curves 4 and 5 Y is $\ln(-\ln(V)/p_b C)$: 1–3 curves, TOAC-4 bound to the *M. luteus* cell at 77 K, the mean concentration of TOAC-4 in probes is $1.1 \cdot 10^{-4}$ M, $2.0 \cdot 10^{-4}$ M and $2.8 \cdot 10^{-4}$ M, respectively; curve 4, calculated dependence for spin labels located on both surfaces of a spherical layer with $d = 7$ nm and $R = 500$ nm; curve 5, calculated dependence for spin labels located in the bulk of a spherical layer with $d = 2.4$ nm and $R = 500$ nm.

$\langle r \rangle$, the membrane curvature will be small and therefore the spin distribution can be estimated accurately by assuming a planar membrane. The observed deviation from the ideal flat membrane model can arise in two cases, i.e., when the labels are situated randomly orientated in the bulk of the membrane or when they are distributed at both membrane surfaces. Thus, of interest are the model calculations of q for these particular cases.

3.2 Model Calculations

In model calculations, the cell membrane was represented as a spherical layer with thickness d and inner radius R. The two models of the spatial distribution of spin labels in the cell membrane were considered to describe the experimental PELDOR signal dependences on two different kinds of random distributions of spin labels: (i) in the volume of this layer and (ii) on both surfaces of the spherical layer. It was assumed that in both cases, the spin labels are located independently of one another.

The dipole-dipole interaction between spins A and spins B causes a shift in the resonance frequencies of spins A as compared with the frequencies in the absence of the dipole-dipole interaction. The action of the pumping pulse at time T leads to a change in the projection of spins B onto the external magnetic field and therefore to the dependence of resonance frequencies of spins A on time. In the general case, the dependence of spin A frequency on time t, $\omega_A(t)$, can be given as [15]

$$\omega_A(t) = \omega_A + \sum_k \omega_k S_{zk}(t)\,, \tag{2}$$

$$\omega_k(t) = \gamma^2\hbar\frac{1-3\cos^2(\theta_k)}{r_k^3}\,, \tag{3}$$

where ω_A is the spin A frequency in the absence of coupling with spins B; $\omega_k(t)$ is the shift of the spin A frequency due to the coupling with the k-th spin B; $S_{zk}(t)$ is the value of k-th spin B projection onto the external magnetic field; r_k is the distance between spin A and the k-th spin B; θ_k is the angle between the vector r_k and the external magnetic field.

According to ref. 17, when the spin frequency depends on time, the spin echo signal density is of the form

$$V = \langle\langle\exp(-\mathrm{i}\int_0^{2\tau} s(t)\omega_A(t)\,\mathrm{d}t)\rangle_t\rangle_{AB}\,, \tag{4}$$

where $\langle\ldots\rangle_t\rangle_{AB}$ is the averaging over all realizations of the accidental process of frequency dependence on time t and the averaging over all realizations of the spatial distribution of spins B with respect to spins A; $s(t) = 1$ at $0 < t < \tau$ and $s(t) = -1$ at $0 < t < 2\tau$.

In case of the PELDOR technique, the time dependence of the frequencies of spins of type A is rather simple. Under the action of the pumping pulse, at $t = T$, the projection of spins B onto the magnetic field direction changes with the probability p_b. Thus, the S_{zk} values, having the equiprobable value of $\pm 1/2$ at $t < T$, change their sign at $t = T$ with the probability p_b and preserve it at $t > T$. When the spin-lattice relaxation time of spins B is much greater than 2τ, the other possibilities of a change in the projections of spins B as compared with the action of the pumping pulse can be neglected. In this case, with respect to Eq. (2), averaging Eq. (4) over time gives

$$\begin{aligned} V &= \langle\langle\exp(-\mathrm{i}\sum_k \omega_k \int_0^{2\tau} s(t)S_{zk}(t)\,\mathrm{d}t)\rangle_t\rangle_{AB} \\ &= \langle\langle\exp(-\mathrm{i}\sum_k \omega_k T S_k)\rangle_{S_k}\rangle_{AB}\,, \end{aligned} \tag{5}$$

where $S_k = +1$ or -1 is the k-th projection of spin B after the action of the pumping pulse. Note that with the averaging over a great number of spins A, the imaginary part of Eq. (5) tends to zero.

Equation (5) was used to calculate $V(T)$ by the Monte-Carlo technique. The value of the cell radius R was varied from 250 to 1500 nm. The concentration of spin labels C, i.e., the ratio between the number of labels per one cell N and the cell surface $4\pi R^2$ was varied in the range of $0.5 \cdot 10^{12}$ to $5 \cdot 10^{12}$ cm^{-2}, corresponding to the experimental concentration values. For the probability of spin B rotation by the pumping pulse, we used the above value $p_b = 0.17$. The calculated results show that in the range of the experimental T values, the $V(T)$ dependence can be given for both cases of spin label distribution as

$$V = \exp(-\beta p_b C T^q), \tag{6}$$

where β and q are the calculated parameters, p_b is the probability of spin B rotation by the pumping pulse, C is the concentration of spin labels, $C = N/4\pi R^2$.

Equation (6) coincides with the empirical dependence Eq. (1) for $\alpha = \beta p_b C$. Figure 4 gives the calculated dependences of $\ln[\ln(V)/p_b C]$ on $\ln(T)$ for $R = 500$ nm, corresponding to the maximum of the *M. luteus* size distribution function which exemplifies the validity of Eq. (6). Curve 4 was obtained for a spin label distribution on both surfaces of the spherical layer with thickness $d = 7.0$ nm. Curve 5 refers to the location of labels in the volume of a spherical layer with thickness $d = 2.4$ nm. The points are the values calculated for $C = 0.5 \cdot 10^{12}$, $1 \cdot 10^{12}$ and $5.0 \cdot 10^{12}$ cm^{-2}. The lines are drawn through the mean values. As follows from Fig. 4, in the given coordinates, the dependencies are linear, which confirms that Eq. (6) is valid. Similar dependences were derived for other d values for both of the models. The β and q values were obtained from the parameters of calculated lines in the given coordinates. The calculated β and q appeared to depend on the layer thickness and to be independent of the $p_b C$ value.

Note that the q value is more convenient for comparing calculations with the experiment than the parameter β because the q value is found just from the inclination angle of the experimental line in the coordinates $\ln(\ln(V))$ vs. $\ln(T)$. To get the experimental value for β, according to Eq. (6), the experimental values for p_b and C are necessary to be known to sufficient accuracy. This makes it difficult to determine the β value within necessary accuracy.

Figure 5 shows the calculated dependences of the parameter q on the thickness of layer d for both cases of spin label distributions. Curve 1 in Fig. 5 was obtained for the location of the spin labels in the bulk of the membrane. Curve 2 refers to the location of labels on both surfaces of the spherical layer. When $d = 0$, in both cases $q = 0.66$, which actually coincides with the value of 2/3 obtained earlier in ref. 18 for a spin distribution at the surface. In the case of the bulk spin label distribution (curve 1), the q value monotonously increases with the layer thickness d and tends to $q = 1$ typical of the unlimited volume. In contrast, curve 2 referring to spin label distributions on both membrane surfaces, passes through a maximum with increasing d and tends to

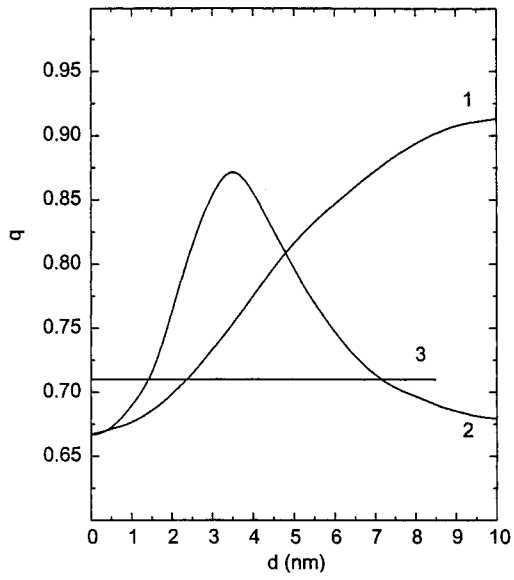

Fig. 5. Calculated dependences of the parameter q on the spherical layer thickness d with $R = 500$ nm. Curve 1, the q dependence for labels located in the bulk of the layer. Curve 2, the q dependence for labels located on both surfaces of the layer. Curve 3, the experimental value $q = 0.71 \pm 0.012$.

a value of 2/3 corresponding to a distribution at largely separated surfaces when the coupling of spins between the different surfaces can be neglected. The maximum in curve 2 is likely to correspond to a distance between spin labels where the dipole-dipole relaxation would be most effective at the experimental T range.

As has been mentioned, the cell radius is large enough to consider a flat cell membrane with inner and outer surfaces separated by about 8 nm. In this case, the calculated results should depend only weakly on R. Similar calculations for other R values within the range of 250 to 1500 nm and for the ideally flat case ($R = \infty$) give curves almost coinciding with dependences 1 and 2 shown in Fig. 5 and obtained at $R = 500$ nm.

4 Discussion

The experimental dependences of $\ln(V)$ versus T for TOAC-4 bound to *M. luteus* cells (see Fig. 3) does not show the characteristic features that have been observed in aggregates of this compound formed in hydrophobic solvents at a concentration of about 0.5 mM [8]. This means that trichogin in its membrane-bound form does not form aggregates at the microscopic concentration of at least 8 mM. In this respect it is of interest to note that this concentration falls in the range

in which trichogin has been shown to induce ion conduction through membranes of large unilamellar vesicles of L-α-phosphatidylcholine [19].

Line 3 in Fig. 5 corresponds to the experimental value $q = 0.71 \pm 0.012$. It crosses the calculated curves 1 and 2. The intersection points provide d values for the two different label distribution models in the membrane. There are two types of solutions: at low d values line 3 crosses both curves 1 and 2; at a high d value line 3 intersects curve 2 only.

The intersection of line 3 with curve 1 at $d = 2.4 \pm 0.3$ nm means that the experimental data are in agreement with a distribution of spin labels in a volume of the layer of this thickness. However, the obtained value of $d = 2.4$ nm is too small in comparison with the membrane thickness (7.5 nm) and cell wall (20–40 nm) [20, 21]. This result shows that the spin labels could not uniformly occupy the full volume of the membrane or cell wall but only some part of them. The obtained small thickness of the layer denotes that the spin labels are placed near a flat surface. One of the possible models of spin label displacement in this case is the random distribution of spin labels inside the thin layer close to the outer surface of either membrane or cell wall.

The intersections of line 3 with curve 2 in Fig. 5 correspond to a distribution of spin labels on both surfaces of the layer. The first is crossing at $d = 1.5 \pm 0.2$ nm. This value of d is too small in comparison with the approximately known membrane or wall thickness and this type of spin label distribution seems not realistic.

The intersection of curve 3 with curve 2 at high d corresponds to a distance $d = 7.0 \pm 0.3$ nm between surfaces on which the spin labels are located. This value corresponds to a location of spin labels at both (external and internal) surfaces and is in a good agreement with the up-to-date concepts of the membrane thickness of *M. luteus* cells. Note that the obtained value $d = 7$ nm is in excellent agreement with the literature data on the membrane thickness (7.5 nm; [20–22]).

Assuming that the average membrane thickness in *M. luteus* is determined by the major lipid constituent (cardiolipin, a phospholipid containing C18:0C18:1 fatty acyl side chains [23, 24]) one would expect a thickness of 4.3–4.5 nm [25]. However, membrane proteins tower above the plane of the lipid bilayer and increase the overall diameter of biomembranes to about 6–8 nm [22]. Thus, trichogin molecules may preferentially bind to bulging membrane proteins instead of phospholipids.

As we have dicussed before, the comparison between the experimental and calculated data shows that the spin-labeled peptides studied are mainly situated near the membrane surface. In this case, two variants of peptide locations are possible: (i) in the layer just below of the outer membrane surface with a spread in distances between the spin labels of about 2.4 nm; (ii) at both inner and outer surfaces with a distance between the surfaces of about 7 nm.

The calculated values of the β parameter allow one to use the experimental values of α and p_b to estimate the effective concentrations of spin labels $C = \alpha/(\beta p_b)$ in the framework of both models (the real surface concentration

is $C_s = C/2$ and the real bulk concentration is $C_v = C/d$). The value of β for the bulk model at $d = 2.4$ nm is $2.74 \cdot 10^{-8}$ $s^{-q}cm^2$, whereas for the distribution model at both surfaces $\beta = 1.59 \cdot 10^{-8}$ $s^{-q}cm^2$. The a value determined from dependences 1–3 in Fig. 4 varies from $0.4 \cdot 10^4$ to $1.3 \cdot 10^4$ $s^{-0.71}$. The experimental value of p_b is 0.17. With these data, the range of experimental concentration values $0.86 \cdot 10^{12}$ $cm^{-2} < C < 2.8 \cdot 10^{12}$ cm^{-2} is obtained for the bulk model and $1.48 \cdot 10^{12}$ $cm^{-2} < C < 4.8 \cdot 10^{12}$ cm^{-2} for the two spherical surfaces. Thus, depending on the model studied, the mean distance between spin labels can be within the range of 4.5 to 10 nm. This finding favors a low degree of surface filling with peptide molecules.

The question is still to be answered whether trichogin molecules preferentially bind to the membrane or cell wall. From the work of Letellier and coworkers [12, 13] we know that in the membrane of *M. luteus* K^+-ATPase pumps are active in maintaining a high K^+-concentration inside the cell cytoplasm. Thus, the efflux of K^+ ions after treatment of cells with trichogin would indicate that trichogin is capable to diffuse through the cell wall and to target the membrane. Indeed, experiments in our laboratory show the release of K^+ ions upon binding of trichogin GA IV to *M. luteus* cells. However, it is not yet clear whether the increase of the ion permeability is due to an ion conduction mechanism, like it has been observed in liposomes [19], or to a blockage of the K^+-ATPase pump function. Nevertheless, it is evident that trichogin molecules are capable to diffuse through the rather porous cell wall to attack the cytoplasmic membrane (including the membrane-bound proteins). Thus, one of the models discussed above, wherein trichogin molecules are supposed to be distributed in a thin layer just

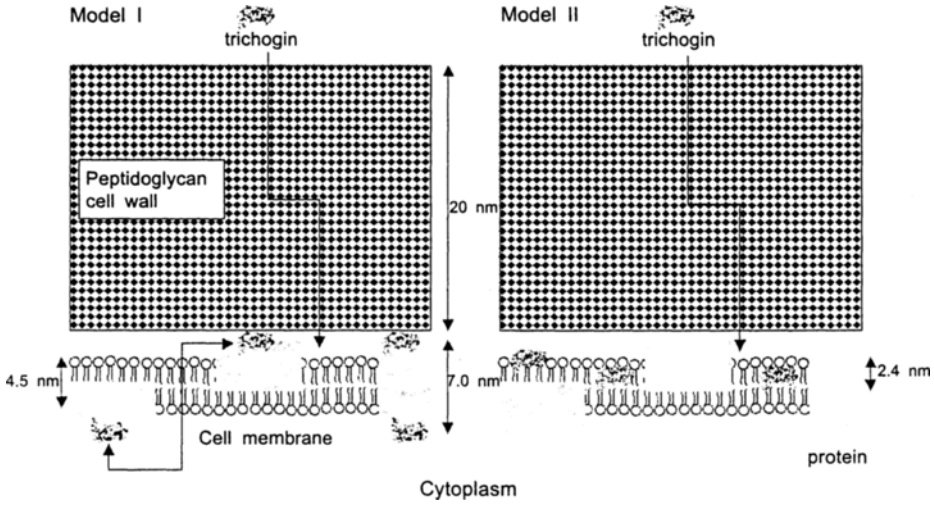

Fig. 6. Two different binding modes of trichogin GA IV to *Micrococcus luteus* cells: trichogin molecules bound to bulging membrane proteins at both sides of the double layer, model I; the periplasmic side of the membrane and distributed into a layer of 2.4 nm thickness, model II.

below the outer cell wall, can be excluded. By combining both the ESR and PELDOR and ion conductivity data we conclude that trichogin molecules are bound to the membrane and not to the cell wall. The different binding models of trichogin to the cell are shown in Fig. 6.

5 Conclusions

It is shown that the method of double resonance in electron spin echo can be used to study the peculiarities of the distribution of spin-labeled molecules in cell membranes.

The data obtained for the phase relaxation of spin labels for spin-labeled trichogin bound to frozen *M. luteus* cells exclude the possibility of membrane-bound aggregates. The main target of the peptaibol after penetration of the porous cell wall is the phospholipid cytosolic membrane. Two different models of peptide distributions are proposed for this bilayer: (i) a random distribution on both inner and outer surfaces of the membrane at a distance between the surfaces of 7 nm; (ii) a random distribution in a ca. 2.4 nm thick layer below the outer surface. Whether the peptide molecules are bound to phospholids (cardiolipin and phosphatidyl glycerol are the major constituents [23, 24]) or membrane proteins (49% w.w. of the membrane [20]) is not clear yet and will be the subject for further studies.

Acknowledgements

We are thankful to J. V. Surovtsev and A. N. Shvalov for measurements performed by the FLSI method and for Dr. T. N. Kropacheva (Chemistry Department, Udmurt State University, Izhevsk, Russia) for the measurements of trichogin-induced K^+ efflux through the bacterial membrane of *M. luteus* cells.

The research described in this publication was supported by The Netherlands Organization of Scientific Research (NWO), project 047-006-009 and Russian Foundation for Basic Research, grants 02-03-32022, 00-15-97321 and 00-03-40124.

References

1. Toniolo C., Crisma M., Formaggio F., Peggion C., Epand R.F., Epand R.M.: Cell. Mol. Life Sci. **58**, 1179–1188 (2001)
2. Epand R.F., Epand R.M., Formaggio F., Crisma M., Wu H., Lehrer R.I., Toniolo C.: Eur. J. Biochem. **268**, 703–712 (2001)
3. Auvin-Guette C., Rebuffat S., Prigent Y., Bodo B.: J. Chem. Soc. Perkin Trans. I **1974**, 249–255.
4. Monaco V., Formaggio F., Crisma M., Toniolo C., Hanson P., Millhauser G.: Biopolymers **50**, 239–253 (1999)
5. Monaco V., Formaggio F., Crisma M., Toniolo C., Hanson P., Millhauser G., George C., Deschamps J.R., Flippen-Anderson J.L.: Bioorg. Med. Chem. **7**, 119–131 (1999)
6. Milov A.D., Maryasov A.G., Tsvetkov Yu.D., Raap J.: Chem. Phys. Lett. **303**, 135–143 (1999)

7. Milov A.D., Maryasov A.G., Samoilova R.I., Tsvetkov Yu.D., Raap J., Monaco V., Formaggio F., Crisma M., Toniolo C.: Dokl. Akad. Nauk **370**, 265–268 (2000)
8. Milov A.D., Tsvetkov Yu.D., Formaggio F., Crisma M., Toniolo C., Raap J.: J. Am. Chem. Soc. **122**, 3843–3848 (2000)
9. Milov A.D., Tsvetkov Yu.D., Raap J.: Appl. Magn. Reson. **19**, 215–227 (2000)
10. Milov A.D., Tsvetkov Yu.D., Formaggio F., Crisma M., Toniolo C., Raap J.: J. Am. Chem. Soc. **123**, 3784–3789 (2001)
11. Cociancich S., Grhazi A., Hetru C., Hoffmann J.A., Letellicr L.: J. Biol. Chem. **268**, 19239–19245 (1993)
12. Bourdineaud J.P., Boulanger P., Lazdunski C., Letellier L.: Proc. Natl. Acad. Sci. USA **87**, 1037–1041 (1990)
13. Surovtsev J.V., Rasumov J.A., Nekrasov V.M., Shvalov A.N., Soini J.T., Maltsev V.P., Petrov A.K., Loktev V.B., Chernyshov A.V.: J. Theor. Biol. **200/3**, 407–417 (2000)
14. Anderson D., Hanson P., McNulty J., Millhauser G., Monaco V., Formaggio F., Crisma M., Toniolo C.: J. Am. Chem. Soc. **121**, 6919–6927 (1999)
15. Milov A.D., Maryasov A.G., Tsvetkov Yu.D.: Appl. Magn. Reson. **15**, 107–143 (1998)
16. Milov A.D., Salikhov K.M., Schirov M.D.: Fiz. Tverd. Tela (Leningrad) **23**, 97 (1981)
17. Klauder J.R., Anderson P.V.: Phys. Rev. **125**, 912–930 (1962)
18. Raitsimring A.M., Salikhov K.M.: Bull. Magn. Reson. **7**, 912–930 (1985)
19. Kropacheva T.N., Raap J.: Biochim. Biophys. Acta (2002) in press.
20. Salton M.R.J.: J. Gen. Phys. **52**, 237s (1985)
21. Salton M.R.J.: The Bacterial Cell Wall. Amsterdam: Elsevier 1964.
22. Drews G. in: Procaryote Structure and Function: a New Perspective, Society for General Microbiology, Symposium 47 (Mohan S., Dow C., Cole J.A., ed.), pp. 249–274. New York: Cambridge University Press 1991.
23. Whiteside T.L., Siervo A.J., Salton M.R.J.: J. Bacteriol. **105**, 957–967 (1971)
24. Thorne K.J.I., Kodicek E.: Biochim. Biophys. A **59**, 306–312 (1962)
25. Caffrey M., Feigenson G.W.: Biochemistry **20**, 1949–1961 (1981)

Authors' address: Yurii D. Tsvetkov, Institute of Chemical Kinetics and Combustion, Russian Academy of Sciences, Institutskaya ulitsa 3, 630090 Novosibirsk, Russian Federation